Research Article | Vol. 28, No. 19 / 14 September 2020 / Optics Express 27966
Optics EXPRESS

Quartz-enhanced photoacoustic spectroscopy exploiting a fast and wideband electro-mechanical light modulator

HUADAN ZHENG,[1,2] YIHUA LIU,[1] HAOYANG LIN,[1] RUIFENG KAN,[2,3] LEI DONG,[4,6] WENGUO ZHU,[1] JUNBIN FANG,[1] JIANHUI YU,[1,7] FRANK K TITTEL,[5] AND ZHE CHEN[1]

[1]*Key Laboratory of Optoelectronic Information and Sensing Technologies of Guangdong Higher Education Institutes, Department of Optoelectronic Engineering, Jinan University, Guangzhou 510632, China*
[2]*State Key Laboratory of Applied Optics, Changchun Institute of Optics, Fine Mechanics and Physics, Chinese Academy of Sciences, Changchun 130033, China*
[3]*Key Laboratory of Environmental Optics and Technology, Anhui Institute of Optics and Fine Mechanics, Chinese Academy of Sciences, Hefei 230031, China*
[4]*State Key Laboratory of Quantum Optics and Quantum Optics Devices, Institute of Laser Spectroscopy, Shanxi University, Taiyuan, Shanxi 030006, China*
[5]*Department of Electrical and Computer Engineering, Rice University, Houston, Texas 77005, USA*
[6]*donglei@sxu.edu.cn*
[7]*kensomyu@gmail.com*

Abstract: A quartz-enhanced photoacoustic spectroscopy (QEPAS) gas sensor exploiting a fast and wideband electro-mechanical light modulator was developed. The modulator was designed based on the electro-mechanical effect of a commercial quartz tuning fork (QTF). The laser beam was directed on the edge surface of the QTF prongs. The configuration of the laser beam and the QTF was optimized in detail in order to achieve a modulation efficiency of ~100%. The L-band single wavelength laser diode and a C-band tunable continuous wave laser were used to verify the performance of the developed QTF modulator, respectively, realizing a QEPAS sensor based on amplitude modulation (AM). As proof of concept, the AM-based QEPAS sensor demonstrated a detection limit of 45 ppm for H_2O and 50 ppm for CO_2 with a 1 s integration time respectively.

1. Introduction

Optical gas sensors based on laser spectroscopy have been increasing in recent decades due to the development of laser technology [1–5]. Photoacoustic spectroscopy (PAS) is an advantageous method with two merits: i) the signal amplitude of PAS is proportional to the excitation power and ii) the detection module is not limited by the laser wavelength since a photoelectric detector is not required. PAS has been widely used for environmental monitoring, industrial process control and medical diagnostics [6–10]. As a variance of PAS, quartz-enhanced photoacoustic spectroscopy (QEPAS), which was first demonstrated in 2002 [11] has proved to be a highly sensitive and noise-immune spectroscopic technique for trace gas sensing. Different from conventional PAS, the energy generated by molecular V-T relaxation upon laser absorption was stored in a sharply resonant quartz tuning fork (QTF) [12–20]. The commercially available QTF has a unique resonance frequency of 32,768 Hz, which was originally designed for time keeping in electronics. Benefit from the unique resonance frequency, QEPAS demonstrated excellent capacity of ambient acoustic noise immunity [21–23]. As a result QEPAS achieved a comparable sensitivity as conventional PAS but provides the advantages of an ultra-compact sensor structure, strong noise-immunity and a cost-effective price.

#400100 https://doi.org/10.1364/OE.400100
Journal © 2020 Received 19 Jun 2020; revised 20 Aug 2020; accepted 26 Aug 2020; published 9 Sep 2020

Optics EXPRESS

QEPAS has been demonstrated for detecting dozens of kinds of gas molecules including both resolved narrow-line absorption and unresolved broadband absorption [5,24–26]. For molecules with well-resolved absorption lines, wavelength modulation (WM) and harmonic detection are combined to improve the detection signal to the noise ratio (SNR) [27]. For molecular species with unresolved broad absorption amplitude modulation (AM) and direct detection should be used [28]. A commonly used AM method in PAS is the use of a chopper to modulate the laser beam intensity. The chopper works well in PAS, since the modulation frequency in conventional PAS is often <5 kHz in order to avoid the 1/f noise. However conventional AM technique fails in QEPAS. A chopper offers a modulation frequency of < 10 kHz, such as the best-selling high-speed optical chopper by Thorlabs MC2000 or the Stanford Research System SR540. The modulation frequency of QEPAS reached as high as 32 kHz which is more than 6 times that of a mechanical optical chopper. Electro-optical modulator (EOM) is an option for high-frequency optical modulation. However the input optical power of the EOM is often limited to hundreds of milliwatt due to the power-handling capacity of the associated crystal [29]. As the PAS signal is proportional to the excitation power, the limited optical power will reduce the photoacoustic detection sensitivity [30]. Moreover, the EOM usually has a specified working wavelength range limit with several hundred nanometers. The much larger size of an EOM is not consistent with the small QTF thereby destroying the compactness of QEPAS.

Although for light sources such as light emitting diodes (LEDs) or solid-state lasers, the AM technique can be achieved by modulation of the injection current [31,32]. However, for many other sources such as external-cavity lasers or optical parametric oscillator (OPO) lasers, the high modulation frequency and large modulation depth are a big challenge for AM modulation due to mode hopping.

In this paper, we introduced a novel and effective AM technique for quartz enhanced photoacoustic spectroscopy. A fast and wideband electro-mechanical light modulator was designed based on a commercially available QTF. A sine electrical signal was applied to the QTF in order to drive its prongs to convert the continuous laser wave into pulses. The prong displacement caused by the periodic electrical signal periodically blocks the light beam thereby realizing AM modulation. The position effect in the configuration of the QTF modulator was optimized to achieve a modulation efficiency of ~100%. A 1.57 μm (L-band) single wavelength laser diode and a 1.37 μm (C-band) tunable distributed feedback (DFB) laser were used to verify the AM modulation, respectively. Different concentrations of CO_2 and atmospheric H_2O detection confirmed the good performance of the reported novel AM technique.

2. Design and optimization of QTF modulator

For the AM technique the modulation efficiency is an important characteristic of the modulator. Here, we define the modulation efficiency as η. Figure 1 shows the diagram of modulated sine wave function in rectangular coordinates. The x-axis represents time and the y-axis represents the light intensity. Point A and B are the peaks of the sine wave. The modulation efficiency η which describes the "depth" of the modulation can be given by the following equation:

$$\eta = y_0/y_1 \tag{1}$$

where y_1 is the value of peak intensity and y_0 is the value of peak to peak intensity.

The schematic of the QTF modulator is shown in Fig. 2(a). Due to the electro-mechanical effects of the quartz crystal, the prongs of the QTF will move back and forth to chop the continuous laser beam when a driver voltage was applied to the QTFs pins. Equation (2) describes the point displacement S of the QTF prongs [33]:

$$S = A\left\{cosh(kh) - cos(kh) + \frac{sin(kL) - sinh(kL)}{cos(kh) + cosh(kh)}[sinh(kh) - sin(kh)]\right\} \tag{2}$$

Optics EXPRESS

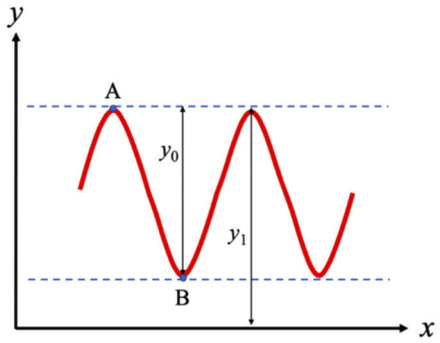

Fig. 1. Definition of laser intensity modulation efficiency.

where A is the normalized amplitude, L is the prong length of the QTF, h is the distance from the point to the QTF basis. The QTF prong length L as measured by a stereoscopic microscope is ~3.8 mm. With respect to its fundamental response frequency of 32768 Hz, the value of kL is equal to 1.875.

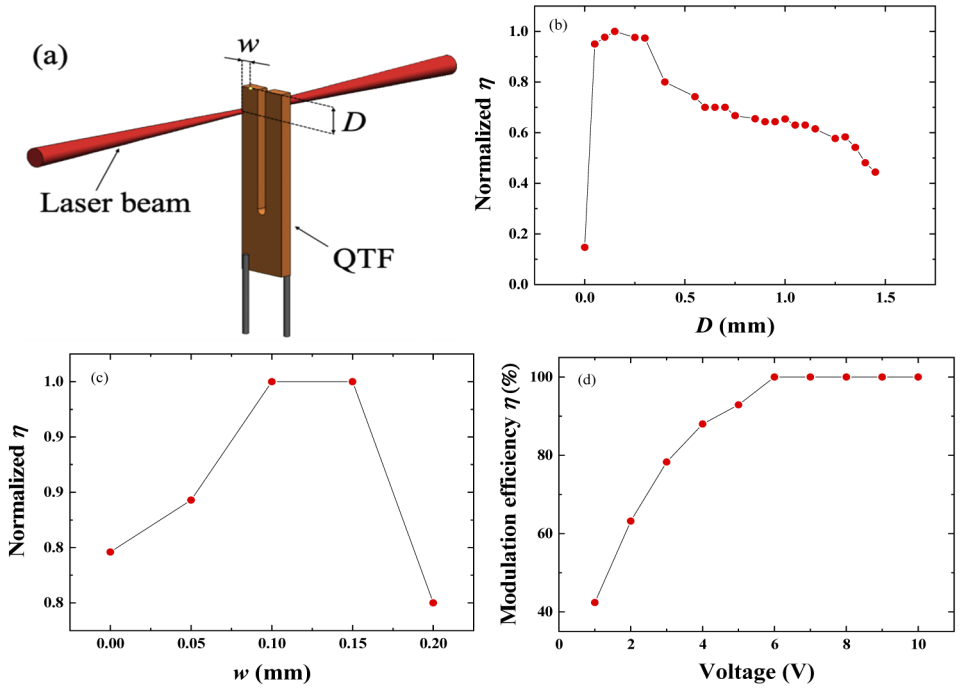

Fig. 2. Optimization of modulation efficiency of the QTF modulator. (a)schematic diagram; (b), (c), (d): modulation efficiency as the function of D, w and driven voltage, respectively.

In order to improve the modulation efficiency of the QTF modulator, the configuration of the laser beam and the QTF was optimized. The laser beam spot position with respect to the QTF prong top and edge, which was defined as D and w, are shown in Fig. 2(a). The normalized modulation efficiency as a function of D and w was plotted in Figs. 2(b) and (c), respectively. The normalized modulation efficiency increased dramatically from D=0 mm to D=0.15 mm. After D=0.15 mm, the normalized modulation efficiency η decreased monotonously by increasing

Optics EXPRESS

of D. For photoacoustic spectroscopy, the PAS signal was proportional to the modulated light power, not the total power of the source [34]. In order to obtain higher modulation efficiency and reduce the background noise, laser was completely switch off during the amplitude modulation. As a result, the laser beam was aligned to be blocked by the QTF prong in the initial position. For the abovementioned reasons, the optimum value for D and w were determined by the beam diameter of 0.15 mm. The electrical signal applied to the QTF pin was increased in order to improve the excitation of the drive signal. With the drive voltage increasing from 1 V to 6 V, the focused laser spot was positioned at the optimum position (D=0.15 mm w=0.15 mm) to achieve a ~100% modulation efficiency. The laser beam went through the QTF modulator (QTF1 in Fig. 4) and then collimated by the window embedded in the gas enclosure. The modulation efficiency η increased from 42.4% to ~100%, indicating that the light beam was completely cut off. With the drive voltage further increased to 10 V, the modulation efficiency η was kept at ~100%. Figure 3 depicts the modulated signal waveform of the QTF modulator. With an optimum configuration of D=0.15 mm, w=0.15 mm and voltage=6 V, a signal period of 30.52 μs was obtained, corresponding to a frequency of 32765 Hz.

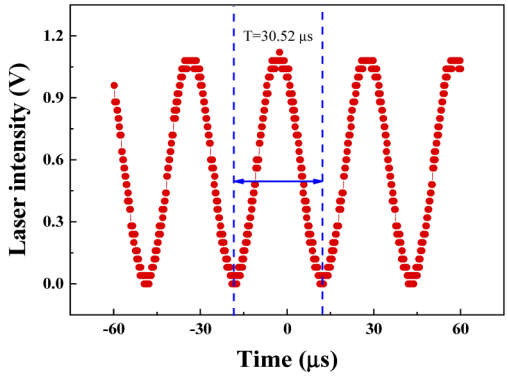

Fig. 3. Signal waveform obtained by the developed QTF modulator.

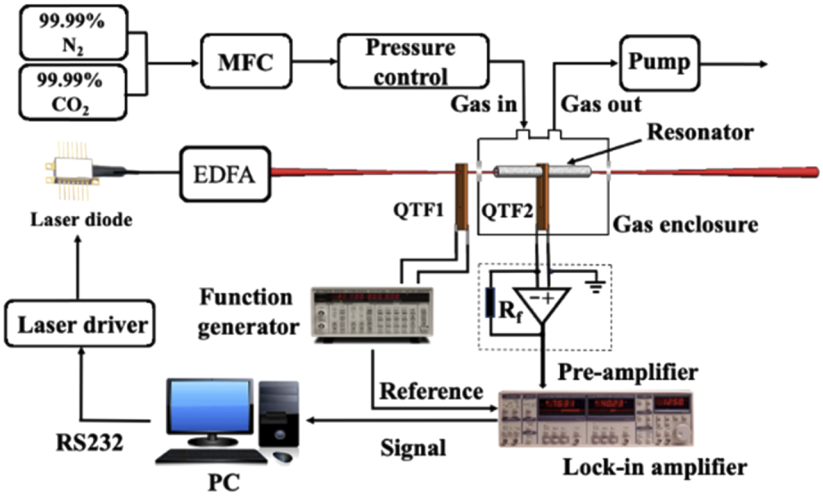

Fig. 4. QEPAS sensor system based on the developed QTF modulator. MFC: mass flow controller; EDFA: erbium doped optical fiber amplifier; PC: personal computer.

Optics EXPRESS

3. Experimental setup

To verify the feasibility of the modulator, a QEPAS gas sensing system was set up by exploiting the AM technique. As proof of concept, the L-band single wavelength laser and a C-band DFB laser were used as excitation light sources to verify the sensor performance, respectively. The schematic of QEPAS sensor system based on the developed QTF modulator is depicted in Fig. 4. The gas stream from two cylinders was fed to the mass flow controller (MFC) system to obtain gas mixture with different concentrations. Vacuum pump (KNF Laboport) and pressure controllers (MKS Instruments) were used to control the pressure of the gas stream. The laser power of the diode was boosted by an erbium doped optical fiber amplifier (EDFA). The amplified laser was focused by a fiber focuser (OZ Optics). The spectrophone was formed by QTF2 and a pair of acoustic micro resonators (AmRs).

The used micro tubes are 4.4 mm in length, 0.6 mm in inner diameter and coupled in an on-beam configuration to enhance the photoacoustic signal amplitude [35]. The sine electric excitation from a function generator (Standford Research System DS345) with an optimized voltage of 6 V was introduced to QTF1 in order to drive its motion. A custom transimpedance preamplifier with a feedback resistance of 10 MΩ was employed to amplify the signals from the QTF2. A lock-in amplifier (Stanford Research Systems, SR830) was operated in the first harmonic mode to demodulate the signal processed by the preamplifier. QTF1 and QTF2 have the same resonance frequency of 32765 Hz. Since the QTF parameters as a mechanical oscillator can be corresponded to equivalent electrical parameters of a series RLC circuit [36]. The slight divergency in resonance frequency can be compensated by adding adjustable capacitors or inductors to the QTF pins. The synchronous port of lock-in amplifier was connected to the TTL output of the function generator. A personal computer (PC) with LabView-based software was used for data processing and retrieving the gas concentrations.

4. Sensor evaluation

4.1. Single wavelength laser diode

An 1.57 μm (L-band) single wavelength laser diode was used to target a CO_2 absorption line. According to the HITRAN database [37], a CO_2 absorption line located at 6361.25 cm^{-1} with the intensity of 1.74×10^{-23} cm/molecule can be targeted. CO_2 with concentrations ranging from 10% to 100% were fed to the QEPAS sensor. The gas stream was controlled at a flow rate of 100 (standard cubic centimeter per minute) SCCM and pressure of 762 Torr. The QEPAS signal amplitudes as the function of CO_2 concentrations were plotted in Fig. 5(a). Each concentration of CO_2 was measured 5 times to evaluate the stability of the sensor system. The noise was measured by filling the gas cell with pure N_2, obtaining an averaged noise level of 8.12×10^{-6} V with a 1σ standard deviation of 1.91×10^{-6} V. Considering 10% CO_2 with a signal level of 3.82×10^{-3} V, the detection SNR was calculated to be ~2000. As a result, the detection limit for CO_2 was 50 ppm with a 1 s integration time. Linear fitting was performed with the data averaged by each concentration as shown in Fig. 5(b). The obtained R square value of 0.996 confirms the good linearity of the developed sensor system.

4.2. Tunable distributed feedback laser

A 1.37 μm (C-band) tunable distributed feedback (DFB) laser was used to detect H_2O in ambient air. Due to the small difference in laser beam spot with 1.57 μm, the laser should be aligned carefully. With the laser temperature controlled at 17.5 °C, the laser injection current was scanned from 42 mA to 58 mA and the H_2O absorption line located at 7194.8 cm^{-1} with an intensity of 3.07×10^{-21} cm/molecule was covered. The H_2O concentration in ambient air of 1.8% was verified by direct absorption spectroscopy as reported in our previous publication [38]. According to the plotted curve depicted in Fig. 6(a) a signal peak of 9.37×10^{-4} V was obtained.

Optics EXPRESS

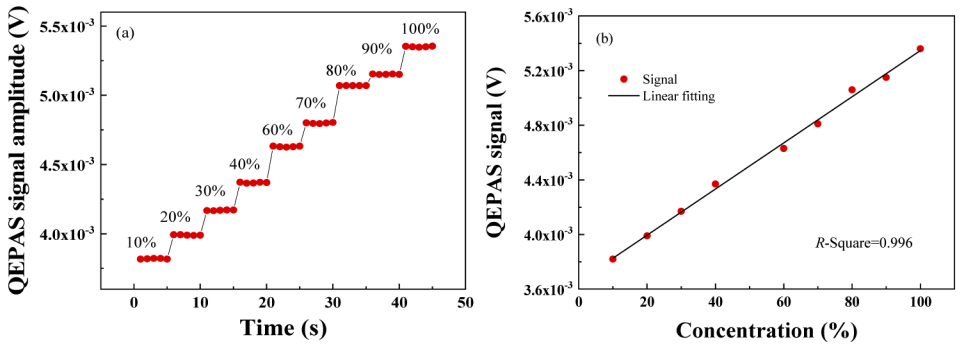

Fig. 5. (a) QEPAS signal as the function of CO_2 concentrations, (b) Linearity of the sensor.

The noise level of the sensor was obtained with a laser injection current of 30~33 mA, where the laser wavelength was far away from the H_2O absorption line. According to Fig. 6(b), a standard deviation of 2.3×10^{-6} V was obtained, corresponding to a detection SNR of ~ 400. As a result, a detection limit of 45 ppm for H_2O was achieved with an1 s integration time.

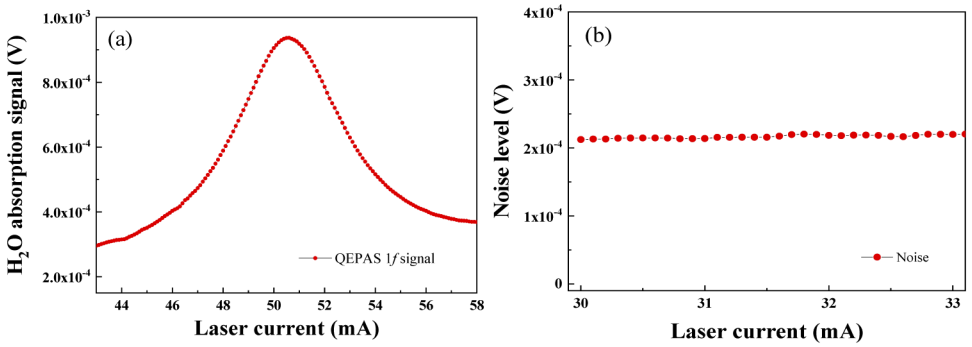

Fig. 6. Detection of H_2O in ambient air.

5. Conclusions

In this paper a novel AM technique for QEPAS was realized based on a QTF modulator. The QTF modulator shows the characteristics of a fast, high extinction ratio and wideband. The modulation frequency of the QTF modulator reached 32 kHz, which is three times faster than that of the mechanical chopper. With an optimized configuration, the maximum extinction ratio was ~100%. Compared to the ultra-fast modulators based on electrical-optical effects and acousto-optical effects, the developed QTF modulator has wider working wavelength range and higher saturation optical power.

AM-based QEPAS sensors were verified by employing the L-band 1.57 μm single wavelength laser diode and a C-band 1.37 μm tunable distributed feedback laser, respectively. As compared with previous publications on CO_2 and H_2O detection based on a QEPAS sensor by using of a wavelength modulation technique [5], the obtained detection sensitivity was comparable. The noise can be attributed to the interference from the leaking chopping noise and the stray light modulated in intensity. However, for light sources where WM modulation cannot be used, such as a QTF modulator opens new horizons. Further improvement can be done by using QTFs with different resonance frequencies from several kHz to hundreds of kHz.

Optics EXPRESS

Funding

National Key Research and Development Program of China (2018YFB1801900); National Natural Science Foundation of China (61675092, 61705086, 61601404, 61771222, 6200031106); Natural Science Foundation of Guangdong Province (2020B1515020024, 2016A030313079, 2016A030311019, 2017A030313375, 2019A1515011380); Key-Area Research and Development Program of Guangdong Province (2019B010138004, 2017A010102006, 2015B010125007); Leading Talents Program of Guangdong Province (CXLJTD-201607); Guangzhou Municipal Science and Technology Project (2016B010111003, 201707010396); Chinese Aeronautical Establishment (201708W4001, 201808W4001); Ministry of Education of the People's Republic of China (6141A02022124); Open foundation of CEPREI (NO. 19D09); Foundation for Distinguished Young Talents in Higher Education of Guangdong (2018KQNCX009); Fundamental Research Funds for the Central Universities (21619402, 11618413); State Key Laboratory of Applied Optics (SKLAO-201914); Science and Technology Planning Project of Shenzhen Municipality (JCYJ20170815145900474); National Science Foundation; American Society for Radiation Oncology (No. R3H685); Welch Foundation (C-0586).

Acknowledgments

Frank Tittel acknowledges the financial support from the US National Science Foundation (NSF) ERC MIRTHE award, a NSF NeTS Large "ASTRO" award (No. R3H685) and a grant C-0586 from the Welch Foundation.

Disclosures

The authors declare no conflicts of interest.

References

1. J. Hodgkinson and R. P. Tatam, "Optical gas sensing: a review," Meas. Sci. and Technol. **24**(1), 012004 (2013).
2. R. Bogue, "Detecting gases with light: a review of optical gas sensor technologies," Sensor Rev. **35**(2), 133–140 (2015).
3. R. Cui, L. Dong, H. Wu, W. Chen, and F. K. Tittel, "Generalized optical design of two-spherical-mirror multi-pass cells with dense multi-circle spot patterns," Appl. Phys. Lett. **116**(9), 091103 (2020).
4. C. Zheng, W. Ye, N. P. Sanchez, A. K. Gluszek, A. J. Hudzikowski, C. G. Li, L. Dong, R. J. Griffin, and F. K. Tittel, "Infrared dual-gas CH_4/C_2H_6 sensor using two continuous-wave interband cascade lasers," IEEE Photonic. Tech. L. **28**(21), 2351–2354 (2016).
5. P. Patimisco, G. Scamarcio, and V. Spagnolo, "Quartz-enhanced photoacoustic spectroscopy: a review," Sensors **14**(4), 6165–6206 (2014).
6. M. W. Sigrist, "Trace gas monitoring by laser photoacoustic spectroscopy and related techniques," Rev. Sci. Instrum. **74**(1), 486–490 (2003).
7. A. Miklós, P. Hess, and Z. Bozóki, "Application of acoustic resonators in photoacoustic trace gas analysis and metrology," Rev. Sci. Instrum. **72**(4), 1937–1955 (2001).
8. X. Yin, L. Dong, H. Wu, H. Zheng, W. Ma, L. Zhang, W. Yin, L. Xiao, S. Jia, and F. K. Tittel, "Highly sensitive SO_2 photoacoustic sensor for SF_6 decomposition detection using a compact mW-level diode-pumped solid-state laser emitting at 303 nm," Opt. Express **25**(26), 32581–32590 (2017).
9. J. Li, W. Chen, and B. Yu, "Recent progress on infrared photoacoustic spectroscopy techniques," Appl. Spectrosc. Rev. **46**(6), 440–471 (2011).
10. K. Chen, Z. Yu, Q. Yu, M. Guo, Z. Zhao, C. Qu, Z. Gong, and Y. Yang, "Fast demodulated white-light interferometry-based fiber-optic Fabry–Perot cantilever microphone," Opt. Lett. **43**(14), 3417–3420 (2018).
11. A. A. Kosterev, Y. A. Bakhirkin, R. F. Curl, and F. K. Tittel, "Quartz-enhanced photoacoustic spectroscopy," Opt. Lett. **27**(21), 1902–1904 (2002).
12. M. Giglio, A. Zifarelli, A. Sampaolo, G. Menduni, A. Elefante, R. Blanchard, C. Pfluegl, M. F. Witinski, D. Vakhshoori, H. Wu, V. M. N. Passaro, P. Patimisco, F. K. Tittel, L. Dong, and V. Spagnolo, "Broadband detection of methane and nitrous oxide using a distributed-feedback quantum cascade laser array and quartz-enhanced photoacoustic sensing," Photoacoustics **17**, 100159 (2020).
13. Y. Ma, Y. He, P. Patimisco, A. Sampaolo, S. D. Qiao, X. Yu, F. K. Tittel, and V. Spagnolo, "Ultra-high sensitive trace gas detection based on light-induced thermoelastic spectroscopy and a custom quartz tuning fork," Appl. Phys. Lett. **116**(1), 011103 (2020).

Optics EXPRESS

14. Z. Wang, Q. Wang, Y. L. Ching, C. Wu, G. Zhang, and W. Ren, "A portable low-power QEPAS-based CO_2 isotope sensor using a fiber-coupled interband cascade laser," Sens. and Actuators B Chem. **246**, 710–715 (2017).
15. H. Zheng, Y. Liu, H. Lin, B. Liu, X. Gu, D. Li, B. Huang, Y. Wu, L. Dong, W. Zhu, J. Tang, H. Guan, H. Lu, Y. Zhong, J. Fang, Y. Luo, J. Zhang, J. Yu, Z. Chen, and F. K. Tittel, "Quartz-enhanced photoacoustic spectroscopy employing pilot line manufactured custom tuning forks," Photoacoustics **17**, 100158 (2020).
16. Q. Zhang, J. Chang, Z. Cong, Y. Feng, Z. Wang, and J. Sun, "Scanned-wavelength intra-cavity QEPAS sensor with injection seeding technique for C2H2 detection," Opt. Laser Technol. **120**, 105751 (2019).
17. H. Wu, L. Dong, X. Yin, A. Sampaolo, P. Patimisco, W. Ma, L. Zhang, W. Yin, L. Xiao, V. Spagnolo, and S. Jia, "Atmospheric CH_4 measurement near a landfill using an ICL-based QEPAS sensor with V-T relaxation self-calibration," Sens. Actuators B Chem. **297**, 126753 (2019).
18. S. Li, L. Dong, H. Wu, A. Sampaolo, P. Patimisco, V. Spagnolo, and F. K. Tittel, "Ppb-level quartz-enhanced photoacoustic detection of carbon monoxide exploiting a surface grooved tuning fork," Anal. Chem. **91**(9), 5834–5840 (2019).
19. M. Mordmueller, S. Edelmann, M. Knestel, W. Schade, and U. Willer, "Phase Optimized Photoacoustic Sensing of Gas Mixtures," Appl. Sci. **10**(2), 438 (2020).
20. J. Hayden, B. Baumgartner, and B. Lendl, "Anomalous Humidity Dependence in Photoacoustic Spectroscopy of CO Explained by Kinetic Cooling," Appl. Sci. **10**(3), 843 (2020).
21. P. Patimisco, A. Sampaolo, H. Zheng, L. Dong, F. K. Tittel, and V. Spagnolo, "Quartz–enhanced photoacoustic spectrophones exploiting custom tuning forks: a review," Adv. Phys. X **2**(1), 169–187 (2017).
22. K. Liu, X. Guo, H. Yi, W. Chen, W. Zhang, and X. Gao, "Off-beam quartz-enhanced photoacoustic spectroscopy," Opt. lett. **34**(10), 1594–1596 (2009).
23. M. Winkowski and T. Stacewicz, "Low noise, open-source QEPAS system with instrumentation amplifier," Sci. Rep. **9**(1), 1838 (2019).
24. M. Mordmueller, W. Schade, and U. Willer, "QEPAS with electrical co-excitation for photoacoustic measurements in fluctuating background gases," Appl. Phys. B **123**(8), 224 (2017).
25. P. Patimisco, A. Sampaolo, L. Dong, F. K. Tittel, and V. Spagnolo, "Recent advances in quartz enhanced photoacoustic sensing," Appl. Phys. Rev. **5**(1), 011106 (2018).
26. H. Zheng, L. Dong, H. Wu, X. Yin, L. Xiao, S. Jia, R. F. Curl, and F. K. Tittel, "Application of acoustic micro-resonators in quartz-enhanced photoacoustic spectroscopy for trace gas analysis," Chem. Phys. Lett. **691**, 462–472 (2018).
27. P. Patimisco, A. Sampaolo, Y. Bidaux, A. Bismuto, M. Scott, J. Jiang, A. Muller, J. Faist, F. K. Tittel, and V. Spagnolo, "Purely wavelength-and amplitude-modulated quartz-enhanced photoacoustic spectroscopy," Opt. Express **24**(23), 25943–25954 (2016).
28. R. Lewicki, G. Wysocki, A. A. Kosterev, and F. K. Tittel, "QEPAS based detection of broadband absorbing molecules using a widely tunable, cw quantum cascade laser at 8.4 μm," Opt. Express **15**(12), 7357–7366 (2007).
29. S. Barke, M. Trobs, B. Sheard, G. Heinzel, and K. Danzmann, "EOM sideband phase characteristics for the spaceborne gravitational wave detector LISA," Appl. Phys. B **98**(1), 33–39 (2010).
30. H. Wu, L. Dong, H. Zheng, X. Liu, X. Yin, W. Ma, L. Zhang, W. Yin, S. Jia, and F. K. Tittel, "Enhanced near-infrared QEPAS sensor for sub-ppm level H_2S detection by means of a fiber amplified 1582 nm DFB laser," Sens. and Actuators B Chem. **221**, 666–672 (2015).
31. M. Kohring, S. Bottger, U. Willer, and W. Schade, "LED-absorption-QEPAS sensor for biogas plants," Sensors **15**(5), 12092–12102 (2015).
32. H. Zheng, L. Dong, X. Yin, X. Liu, H. Wu, L. Zhang, W. Ma, W. Yin, and S. Jia, "Ppb-level QEPAS NO_2 sensor by use of electrical modulation cancellation method with a high power blue LED," Sens. and Actuators B Chem. **208**, 173–179 (2015).
33. F. K. Tittel, A. Sampaolo, P. Patimisco, L. Dong, A. Geras, T. Starecki, and V. Spagnolo, "Analysis of overtone flexural modes operation in quartz-enhanced photoacoustic spectroscopy," Opt. Express **24**(6), A682–A692 (2016).
34. G. C. Liang, H. H. Liu, A. H. Kung, A. Mohacsi, A. Miklos, and P. Hess, "Photoacoustic Trace Detection of Methane Using Compact Solid-State Lasers," J. Phys. Chem. A **104**(45), 10179–10183 (2000).
35. L. Dong, A. A. Kosterev, D. Thomazy, and F. K. Tittel, "QEPAS spectrophones: design, optimization, and performance," Appl. Phys. B-Lasers O. **100**(3), 627–635 (2010).
36. A. A. Kosterev, F. K. Tittel, D. V. Serebryakov, A. L. Malinovsky, and I. V. Morozov, "Applications of quartz tuning forks in spectroscopic gas sensing," Rev. Sci. Instrum. **76**(4), 043105 (2005).
37. http://hitran.org
38. X. Yin, L. Dong, H. Zheng, X. Liu, H. Wu, Y. Yang, W. Ma, L. Zhang, W. Yin, L. Xiao, and S. Jia, "Impact of humidity on quartz-enhanced photoacoustic spectroscopy based CO detection using a near-IR telecommunication diode laser," Sensors **16**(2), 162 (2016).